This is a preprint, the final version is subject to change, of the American Mineralogist (MSA)
Cite as Authors (Year) Title. American Mineralogist, in press.
(DOI will not work until issue is live.) DOI: http://dx.doi.org/10.2138/am-2017-6252

Revision 2

Structuration under Pressure: Spatial Separation of Inserted Water during Pressure-Induced Hydration in Mesolite

Yonghwi Kim,[†,‡] Jinhyuk Choi,[†,‡] Thomas Vogt,[±] and Yongjae Lee[†,§,*]

[†]Department of Earth System Sciences, Yonsei University, Seoul, 03722, Korea

[±]NanoCenter and Department of Chemistry & Biochemistry, University of South Carolina, Columbia , South Carolina 29208, USA

[§]Center for High Pressure Science and Technology Advanced Research, Shanghai 201203, China

‡These authors contributed equally.

ABSTRACT

In-situ high-pressure single crystal X-ray diffraction studies of mesolite, an aluminosilicate composed of stacks of Na^+-containing natrolite and Ca^{2+}-containing scolecite layers in the ratio of 1:2, showed two discrete steps of pressure-induced hydration (PIH): first H_2O molecules are inserted into the natrolite layers between ~0.5 and ~1.5 GPa and subsequently into the scolecite layers. During the PIH in the natrolite layers, the coordination environment of Na^+ changes from six to seven, the same as that of Ca^{2+} in the scolecite layers. While the natrolite layers behave as in the mineral natrolite, the scolecite layers show different behaviors from the mineral scolecite by adopting the super-hydrated natrolite-type structure at higher pressure, as a larger distortion is not favorable in the 1:2 layered framework. This spatial separation of inserted H_2O during PIH and the growing structural similarity of the two layers result in a weakening of $k \neq 3n$ reflections maintaining

the 1:2 layer configuration. Our study of this unique behavior of mesolite provides a simple model of structuration under pressure, and the implications of our experimental findings are discussed.

Introduction

Structuration describes spatio-chemical heterogeneities in materials which drive chemical and physical processes in pores as well as in extended internal and external surfaces resulting in significantly different structures and properties. Nanoscale assemblies of water have a well-established and important impact on the stability, structure, dynamics, and function of proteins (Bellissent-Funel et al. 2016), in surface electrochemistry (Bockris and Khan, 2013) and mineral dissolution (Zhuravlev, 2000). Ordered and confined assemblies of water and cations in microporous materials are important model systems accessible to DFT calculations (Kremleva, 2013). The structuration of cations and molecules in pores of microporous materials by non-thermal pressure-driven supramolecular assembly has allowed the synthesis of novel functional materials and hybrids which, in some cases, can be stable at ambient conditions. Post-synthetic modifications of the as-synthesized metal-organic framework (MOF) MIL-47V using pressure led to reversible and irreversible pressure-induced exchanges of terephthalic acid template molecules by water and methanol, respectively (Im et al. 2016). After pressure release, methanol molecules not only remain in the MIL-47V pores at ambient conditions and form a new material but can only be removed after heating to 400 °C. More recently, it was shown that pressure can be used to form a unique two-dimensional network of spatially separated ethanol dimers and H_2O tetramers in a hydrophobic all-silica zeolite ferrierite, which can be stabilized at ambient conditions (Arletti et al. 2017). Clearly the fact that the pore topology of the microporous material might become tailored via pressure to allow access for certain molecules is an important mechanism to form new supramolecular assemblies of thermally unstable composites with potentially

new functionalities. Our systematic investigations have shown pressure-induced hydration (PIH) (Lee et al. 2001) depends on both size and charge of the extra-framework cation (EFC) (Seoung et al. 2015). In the case of the small-pore zeolite natrolite (NAT), DFT calculations revealed the energetics behind the different PIH behavior of natrolites containing different monovalent EFC (Kremleva et al. 2013). The choice of EFC and the complex behavior under pressure of the EFC-assemblies provides another way to create new reversible (Lee et al. 2010, 2011, 2013) and irreversible supramolecular structuration in zeolites (Lee et al. 2002; Seoung et al. 2014).

The next challenge is to explore the high-pressure chemistry of microporous materials which contain EFC with different charges. One such material is mesolite ($Na_{5.33}Ca_{5.33}Al_{16}Si_{24}O_{80}$ x 21.33 H_2O, **F***dd2*, *a*=18.4049(8), *b*=56.655(6), *c*=6.5443(4) Å) (Artioli et al. 1986) which can formally be derived from natrolite ($Na_{16}Al_{16}Si_{24}O_{80}$ x 16 H_2O, **F***dd2*, *a*=18.3, *b*=18.6, *c*=6.6 Å) (Smith 1983) by replacing 2/3 of the Na^+ cations by Ca^{2+} and H_2O or from scolecite ($Ca_8Al_{16}Si_{24}O_{80}$ x 24H_2O, **C***c*, *a*=6.516(2), *b*=18.948(3), *c*=9.761(1) Å) (Kvich and Stahl 1985) by replacing 1/3 of Ca^{2+} and H_2O by Na^+ (Figure 1). Natrolite, scolecite, and mesolite are small pore zeolites with the same NAT framework topology composed of T_5O_{10} secondary building units formed by connecting five TO_4 tetrahedra (T = Si, Al) which are subsequently linked along the *c*-axis to form co-called natrolite chains (Smith 1983). A fibre chain rotation angle, ψ, defines the geometry of the helical 8-ring channel in the projected *ab*-plane. The chain rotation angle ψ is defined as the average angle between the quadrilateral sides of the secondary building unit, T_5O_{10}. The smaller ψ observed in the mineral scolecite compared to ψ in the mineral natrolite signifies a more expanded channel. Previous studies on fibrous zeolites demonstrate the flexibility of the NAT framework depending on the external pressure conditions and cation types (Comodi et al. 2002; Gatta et al. 2004; Gatta 2005; Gatta and Lee 2014; Seoung et al 2013, 2015). This work reveals how the structure and pressure-driven transformations of previously

characterized bulk structures change when they are alloyed at the atomic scale. The fortuitous structural relationships between natrolite, scolecite, and mesolite makes this an ideal model system to explore the effects of pressure in the presence of water on pores containing different EFC cations in their extended (natrolite, scolecite) and interfacial atomic structure (mesolite).

Experimental Methods

Single-crystal X-ray diffraction measurements at ambient pressure

The diffraction data from a colorless cuboidal shaped crystal of mesolite (175 x 135 x 30 μm^3) mounted on a loop were collected at ambient pressure and temperature on a Bruker Venture CMOS diffractometer equipped with a graphite-monochromated Mo Kα (λ= 0.71073 Å) radiation source. The data were corrected for Lorentz and polarization effects (SAINT) (Bruker-Nonius 2014), and multi-scan absorption corrections based on equivalent reflections were applied (SADABS) (Sheldrick 2014). The structure was refined by full-matrix least-squares on F^2 (SHELX-XL 2014/7) (Sheldrick 2015). All the non-hydrogen atoms were refined anisotropically, and hydrogen atoms were found by difference map and allowed to be refined isotropically.

Single-crystal X-ray diffraction measurements at high pressure

A colorless cuboidal shaped crystal of mesolite (180 x 150 x 100 μm^3) was loaded in Almax Easylab Diacell Bragg-(S) DAC with a half-opening angle of 45°. The cell is made of Type Ia Diacell design diamonds with 800 μm culet diamond anvils, a tungsten gasket with a hole diameter of 400 μm and beryllium backing plates. A mixture of methanol, ethanol, and H_2O (16:3:1 by volume) was added as a pressure transmitting medium to ensure hydrostaticity. The cell was initially pressurized to 0.47(10) GPa. The diffraction data

from the crystal of mesolite mounted on DAC were collected at 0.47(10) (40 frames for unit cell determination), 0.99(10), 1.46(10), and 2.26(10) GPa. The data were integrated with the program SAINT using dynamic masks (Bruker-Nonius 2014), and multi-scan absorption corrections based on equivalent reflections were applied (SADABS) (Sheldrick 2014). The structure was refined by full-matrix least-squares on F^2 (SHELX-XL 2014/7) (Sheldrick 2015). All the atoms were refined isotropically. Pressure-driven changes in the unit cell lengths and volume are summarized in Table S1 and plotted in Figure S1 and 2, respectively, with the corresponding changes in the diffraction data visualized in Figure 3.

Results and discussion

Mesolite is a 2:1 composite of alternating scolecite and natrolite layers. At ambient pressure, mesolite contains two Na^+ ions and two H_2O molecules in the pores of the natrolite layers, and one Ca^{2+} ions and three H_2O molecules in the scolecite layers. The Na^+ ions are 6-coordinated by four framework oxygen atoms and two oxygen atoms from two H_2O molecules, whereas the Ca^{2+} ions are 7-coordinated by four framework oxygen atoms and three oxygen atoms from three H_2O molecules (Figure 1).

Applying hydrostatic pressure, mesolite shows distinct changes of its unit cell parameters while maintaining its orthorhombic symmetry (Figure S1): from ambient pressure to 0.5(1) GPa, all three unit cell axes contract due to compression of the NAT framework. However, between 0.5(1) GPa and 2.3(1) GPa, the *a*- and *b*-axes increase whereas the *c*-axis continuously decreases. This behavior points to a chemical and structural phase transition changing the rotation angle ψ in the *ab*-plane, previously established as a pressure-induced hydration (PIH, Figure 2) (Lee et al. 2002). To elucidate the structural and chemical transition occurring between 0.5(1) GPa and 2.3(1) GPa, sets of X-ray diffraction data were measured at 0.99(10), 1.46(10), and 2.26(10) GPa (Figure 3).

In mesolite at 0.99(10) GPa, additional H_2O sites (O5W) appear in the natrolite layers, which are partially occupied (37.5%), whereas no additional H_2O molecules are found in the scolecite layers (Table S2 and Figure 4). In the natrolite layers, the coordination geometry of Na^+ ions partially changed from a distorted trigonal prism to a pentagonal bipyramid, the same coordination geometry that Ca^{2+} ions have in the scolecite layers. As observed in the mineral natrolite, the change of ψ during PIH leads to increases of the *a*- and *b*-unit cell axes whereas the *c*-axis slightly decreases (Figure S1).

Further pressure increase up to 1.46(10) GPa results in a complete filling of the additional H_2O site (O5W) and the natrolite layers now contain two Na^+ ions and four H_2O molecules per channel. This is the structure found in the super-hydrated mineral natrolite above 1 GPa. Subsequently, at 2.26 GPa, a new H_2O site (O6W) with 50 % occupancy is found in the scolecite layers (Table S2 and Figure 4), giving rise to a splitting of the original Ca^{2+} site into statistically disordered ones. This assembly now also has the topology of super-hydrated natrolite structure. This is in marked contrast to what happens in the mineral scolecite. The difference of the electron density distributions of the natrolite and scolecite layers in mesolite are now reduced, resulting in a weakening of the $k \neq 3n$ reflections (Figure 3). The better signal-to-noise data of our single crystal data allows us to show that these reflections are still present, albeit much weaker. This allows us to revise our previous conclusions based on X-ray powder diffraction studies where we claimed that during PIH the superlattice *b*-axis is reduced by a 1/3 to a natrolite structure (Lee et al. 2002), similar to what was reported in the dehydration study on mesolite (Ståhl and Hanson 1994). Our new model provides a much more appealing explanation for the reversibility of this phenomenon as it does not require cation diffusion between the two different layer types.

The layers in the mineral scolecite and the scolecite layers in mesolite show different PIH as shown in Figure 4. This can be related to the degree of framework distortion, represented here by the ψ angle change. The natrolite layers in both the mineral natrolite

and mesolite are similar, whereas the scolecite layers in the mineral scolecite and mesolite are quite different at higher pressures. The scolecite layers in the mineral reveal a much higher degree of pressure-induced framework distortion (Figure 2). Up to about 1.5 GPa, the ψ angles of the natrolite and scolecite layers (empty symbols in Figure 2) in the mesolite structure lie between those of the minerals natrolite and scolecite. At higher pressures, the ψ angle of the mineral scolecite then drops near 14° whereas the ones in the mesolite structure remains near 20°. The NAT framework common to the scolecite and natrolite layers in the mesolite structure imposes a limit on how different the ψ angle can be. This explains why the degree of super-hydration in the mineral scolecite is higher than in the scolecite layers of the mesolite structure, i.e., 5 H_2O vs. 4 H_2O per channel (Figures 2 and 4).

We have clarified and revised the mechanism of PIH in mesolite. The spatially separated and reversible 'two-step' PIH of first the natrolite- and then the scolecite-layers with increasing hydrostatic pressure in the presence of H_2O molecules is an example of pressure-driven structuration where initial hydration leads to a layer structure isostructural to the ones observed in super-hydrated natrolite. Subsequent hydration in the scolecite layers of mesolite are different from what we find in the super-hydrated mineral scolecite. Instead it leads to a topology that resembles the one of super-hydrated natrolite. This behavior is imposed by the composite framework limiting the degree of the ψ angle variation in the natrolite and scolecite layers. Hydrostatic pressure minimizes the contrast of electron density distribution present in the two layers of mesolite resulting in a weakening but not disappearance of the $k \neq 3n$ superlattice reflections. This disproves our original conclusion invoking cation diffusion between channels and provides us with a simple system to model PIH in a material with two different cations that displays spatially separated pressure-driven hydration. Such an evolution of distinct coordination states under pressure suggests mesolite to be a unique mineral that might further lead to new and unusual physical and chemical properties.

Pressure-induced hydration (PIH) results in spatial changes of confined H_2O molecules located in pores, curved interfaces, and extended external and internal surfaces. We chose the term "structuration" as we would like to highlight the importance that H_2O molecules confined in the pores of microporous materials have, different structures than found in bulk H_2O and point to the established importance of what is sometimes called 'nanowater' in protein, colloids and membranes structures in structural biology. The fibrous zeolites such as natrolite, scolecite, and mesolite are paradigmatic examples of PIH in aluminosilicates which demonstrate that the internal structuration of water depends on the extra-framework cation present in the pore (Na^+ in natrolite, Ca^{2+} in scoleceite) and that when forming atomic interfaces of scoleceite and natrolite pores at the atomistic scale as present in the mineral mesolite the insertion pressures and structural features are different from those observed in extended bulk scoleceite and natrolite. Up to now PIH has been neglected in any modeling attempts for water transport or their potential implications in seismicity and water cycling. Initial work indicates that these systems are amenable to systematic DFT calculation (Kremleva et al. 2013). It would be important for the geoscience community to take note of pressure-induced hydration (PIH) as a general phenomenon and account for its structural and compositional effects when simulating 'real geochemical systems'.

ACKNOWLEDGMENT

This work was supported by the Global Research Laboratory (NRF-2009-00408) and National Research Laboratory (NRF-2015R1A2A1A01007227) programs of the Korean Ministry of Science, ICT and Planning (MSIP). We also thank the supports by NRF-2016K1A4A3914691 and NRF-2016K1A3A7A09005244 grants. The experiments for this work were supported by the Seoul Western Center of Korea Basic Science Institute (KBSI) at Ewha Women's University in Korea. We thank H. Lee at KBSI for instrumental support.

REFERENCES

Arletti, R., Fois, E., Gigli, L., Vezzalini, G., Quartieri, S., and Tabacchi, G. (2017) Irreversible conversion of a water-ethanol solution into an organized two-dimensional network of alternating supramolecular units in a hydrophobic zeolite under pressure. Angewandte Chemie, 129(8), 2137-2141.

Artioli, G., Smith, J.V., and Pluth, J.J. (1986) X-ray structure refinement of mesolite. Acta Crystallographica Section C: Crystal Structure Communications, 42(8), 937-942.

Bellissent-Funel, M.-C., Hassanali, A., Havenith, M., Henchman, R., Pohl, P., Sterpone, F., van der Spoel, D., Xu, Y., and Garcia, A. E. (2016) Water Determines the Structure and Dynamics of Proteins. Chemical Reviews, 116, 7673-7697.

Bockris, J. O. M., Khan, S. U. (2013) Surface Electrochemistry: A Molecular Level Approach, 1014 p. Springer, New York.

Bruker-Nonius. (2014) Bruker-AXS, Madison, Wisconsin, USA.

Comodi, P., Gatta, G.D., and Zanazzi, P.F. (2002) High-pressure structural behavior of scolecite. European Journal of Mineralogy, 14(3), 567-574.

Gatta, G.D., Ballaran, T.B., Comodi, P., and Zanazzi, P.F. (2004) Comparative compressibility and equation of state of orthorhombic and tetragonal edingtonite. Physics and Chemistry of Minerals, 31(5), 288-298.

Gatta, G.D. (2005) A comparative study of fibrous zeolites under pressure. European Journal of Mineralogy, 17(3), 411-421.

Gatta, G.D., and Lee, Y. (2014) Zeolites at high pressure: A review. Mineralogical Magazine, 78(2), 267-291.

Im, J., Seoung, D., Hwang, G.C., Jun, J.W., Jhung, S.H., Kao, C., Vogt, T., and Lee, Y. (2015) pressure-dependent structural and chemical changes in a metal-organic framework with one-dimensional pore structure. Chemistry of Materials, 28(15), 5336-5341.

Kremleva, A., Vogt, T., and Rösch, N. (2013) monovalent cation-exchanged natrolites and their behavior under pressure. A Computational Study. The Journal of Physical Chemistry C, 117(37), 19020-19030.

Kvich, Å., and Ståhl, K. A neutron diffraction study of the bonding of zeolitic water in scolecite at 20 K. Zeitschrift für Kristallographie-Crystalline Materials, 171(1-4), 141-154.

Lee, Y., Hriljac, J.A., Vogt, T., Parise, J.B., and Artioli, G. (2001) first structural investigation of a super-hydrated zeolite. Journal of the American Chemical Society, 123(50), 12732-12733.

Lee, Y., Vogt, T., Hriljac, J.A., Parise, J.B., Hanson, J.C., and Kim, S.J. (2002a) Non-framework cation migration and irreversible pressure-induced hydration in a zeolite. Nature, 420(6915), 485.

Lee, Y., Vogt, T., Hriljac, J.A., Parise, J.B., and Artioli, G. (2002b) pressure-induced volume expansion of zeolites in the natrolite family. Journal of the American Chemical Society, 124(19), 5466-5475.

Lee, Y., Hriljac, J.A., and Vogt, T. (2010) pressure-induced argon insertion into an auxetic small pore zeolite. The Journal of Physical Chemistry C, 114(15), 6922-6927.

Lee, Y., Liu, D., Seoung, D., Liu, Z., Kao, C., and Vogt, T. (2011) pressure- and heat-induced insertion of co2 into an auxetic small-pore zeolite. Journal of the American Chemical Society, 133(6), 1674-1677.

Lee, Y., Seoung, D., Jang, Y., Vogt, T., and Lee, Y. (2013) pressure-induced hydration and insertion of CO_2 into Ag-natrolite. Chemistry-A European Journal, 19(19), 5806-5811.

Seoung, D., Lee, Y., Kao, C., Vogt, T., and Lee, Y. (2013) Super-hydrated zeolites: Pressure-induced hydration in natrolites. Chemistry-A European Journal, 19(33), 10876-10883.

Seoung, D., Lee, Y., Cynn, H., Park, C., Choi, K., Blom, D.A., Evans, W.J., Kao, C., Vogt, T., and Lee, Y. (2014) Irreversible xenon insertion into a small-pore zeolite at moderate pressures and temperatures. Nature chemistry, 6(9), 835-839.

Seoung, D., Lee, Y., Kao, C., Vogt, T., and Lee, Y. (2015) Two-step pressure-induced superhydration in small pore natrolite with divalent extra-framework cations. Chemistry of Materials, 27(11), 3874-3880.

Sheldrick, G.M. (2014) SADABS, version 2014/4. Bruker AXC Inc., Madison, WI.

Sheldrick, G.M. (2015) Crystal structure refinement with SHELXL. Acta Crystallographica Section C: Structural Chemistry, 71(1), 3-8.

Smith, J.V. (1983) Enumeration of 4-connected 3-dimensional nets and classification of framework silicates: combination of 4-1 chain and 2D nets. Zeitschrift für Kristallographie-Crystalline Materials, 165(1-4), 191-198.

Ståhl, K., and Hanson, J. (1994) Real-time X-ray synchrotron powder diffraction studies of the dehydration processes in scolecite and mesolite. Journal of Applied Crystallography, 27(4), 543-550.

Zhuravlev, L. T. (2000) The surface chemistry of amorphous silica. Zhuravlev model. Colloids and Surfaces A: Physicochemical and Engineering Aspects, 173, 1-38.

Figure Captions

Figure 1. The structures of natrolite, scolecite, and mesolite. Mesolite is shown as a 2:1 composite of alternating scolecite and natrolite layers along the *b*-axis. The regions enveloped with rectangles are the unit cells of natrolite (yellow), scolecite (blue), and mesolite (red). Note that the unit cell of scolecite is viewed along [100] direction, and the others are along [001].

Figure 2. Changes in (a) the unit cell volumes ($Å^3$) and (b) rotation angles of natrolite (Na-NAT), scolecite (Ca-NAT), and mesolite (Na,Ca-NAT) as a function of pressure. The unit cell volumes are normalized to 80 framework oxygens. The change of the number of H_2O molecules per 80 framework oxygens is shown during the PIH.

Figure 3. (a) Simulated powder diffraction patterns of mesolite at different pressures, (b) X-ray diffraction spots with Miller indices of $k \neq 3n$.

Figure 4. Polyhedral representations of mesolite (Na,Ca-NAT), natrolite (Na-NAT) and scolecite (Ca-NAT) as a function of pressure. Yellow, cyan, and red circles indicate Na^+, Ca^{2+}, and oxygen atoms of H_2O. Tetrahedra depict an ordered distribution of Si/Al atoms in the framework.

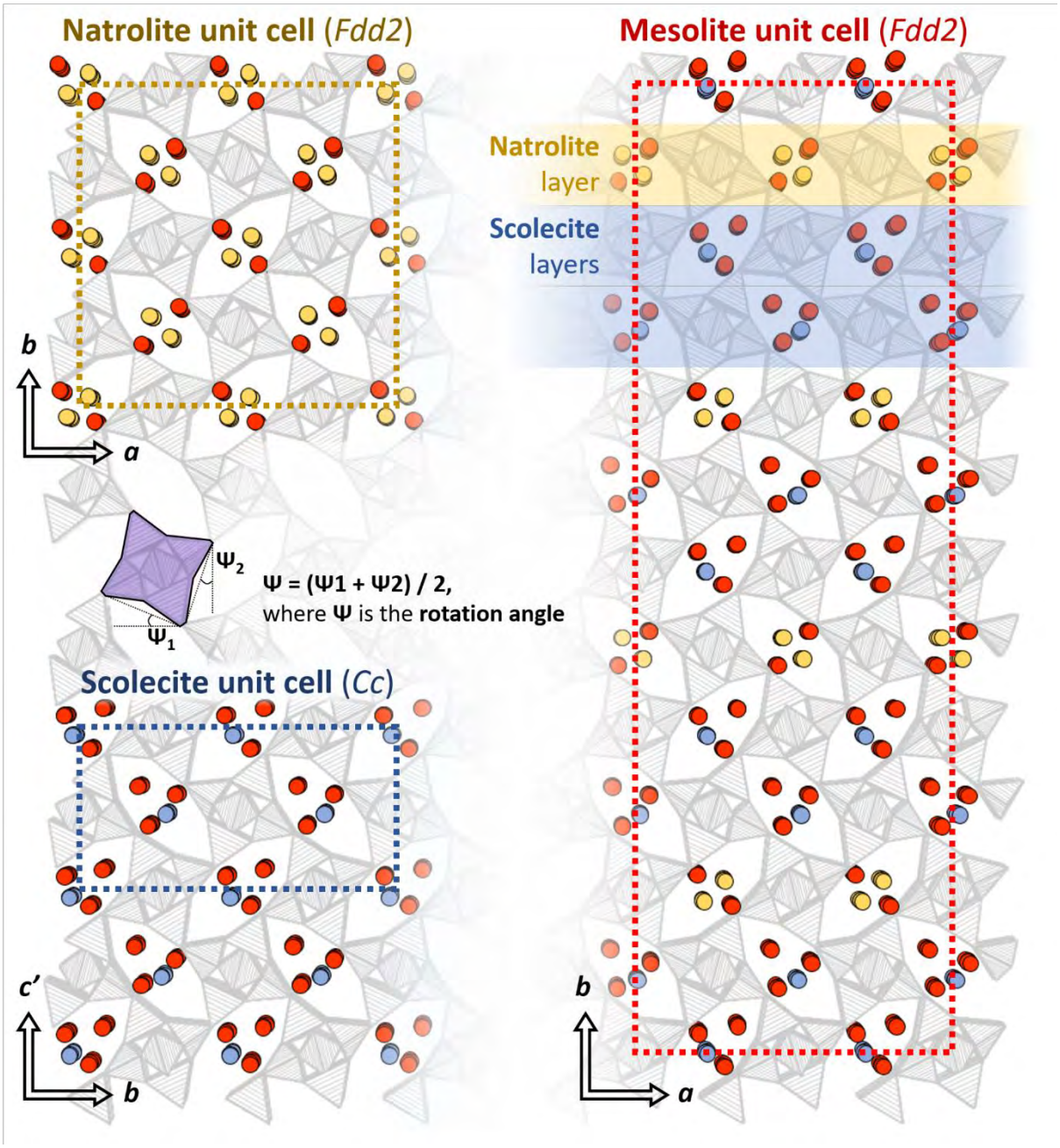

290

291 Fig. 1

292

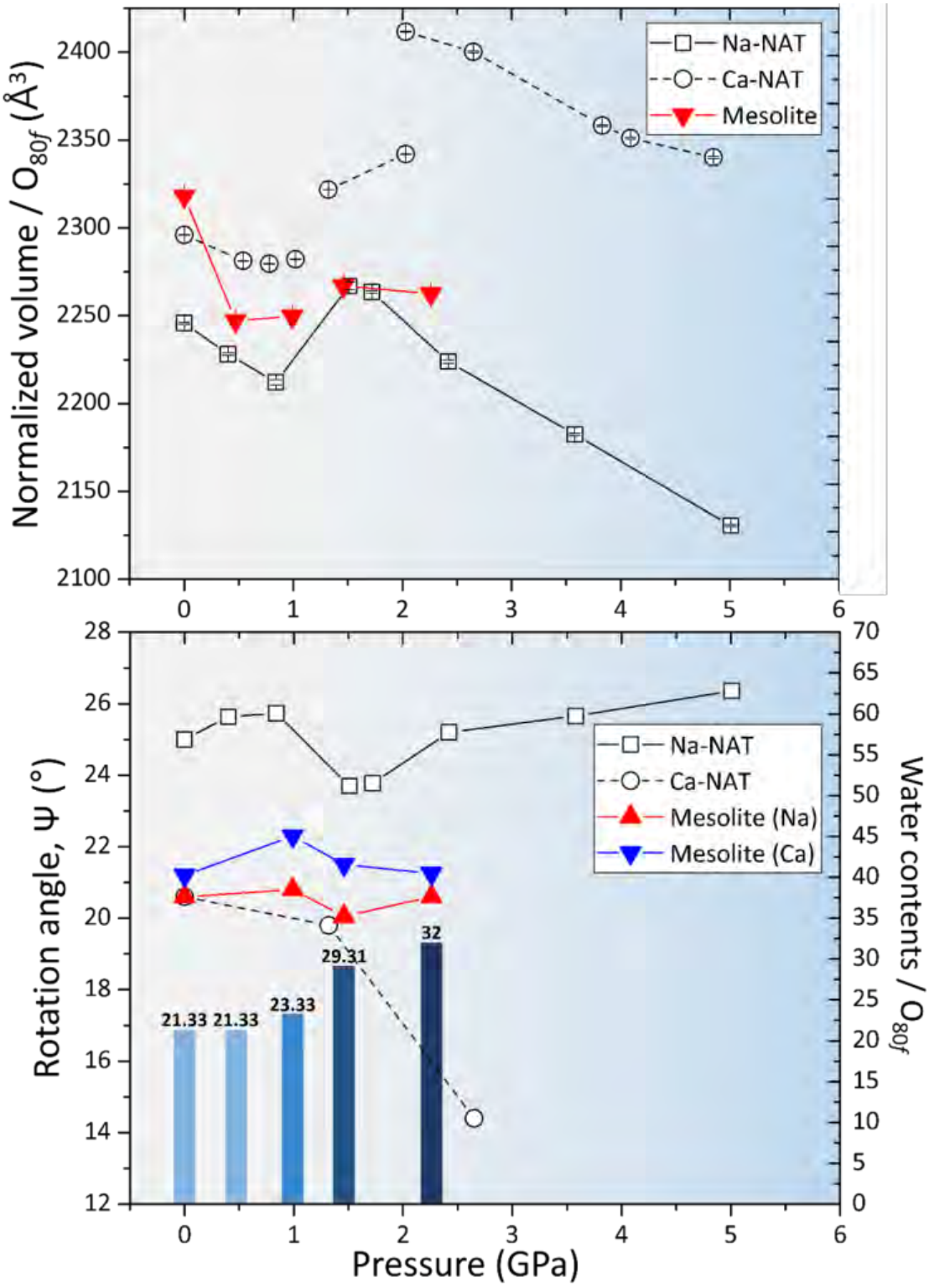

293

294 Fig. 2

This is a preprint, the final version is subject to change, of the American Mineralogist (MSA)
Cite as Authors (Year) Title. American Mineralogist, in press.
(DOI will not work until issue is live.) DOI: http://dx.doi.org/10.2138/am-2017-6252

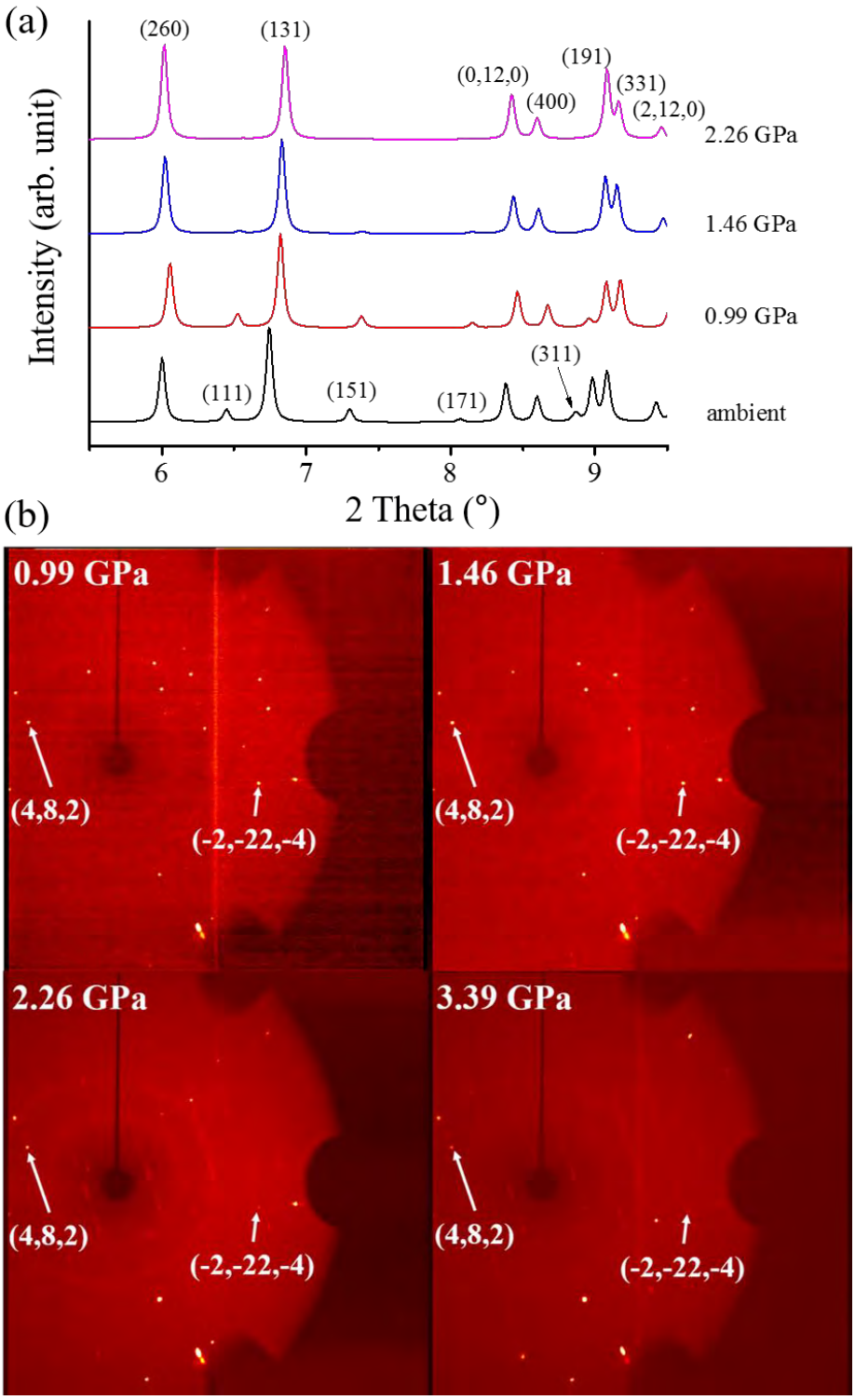

295

296 Fig. 3

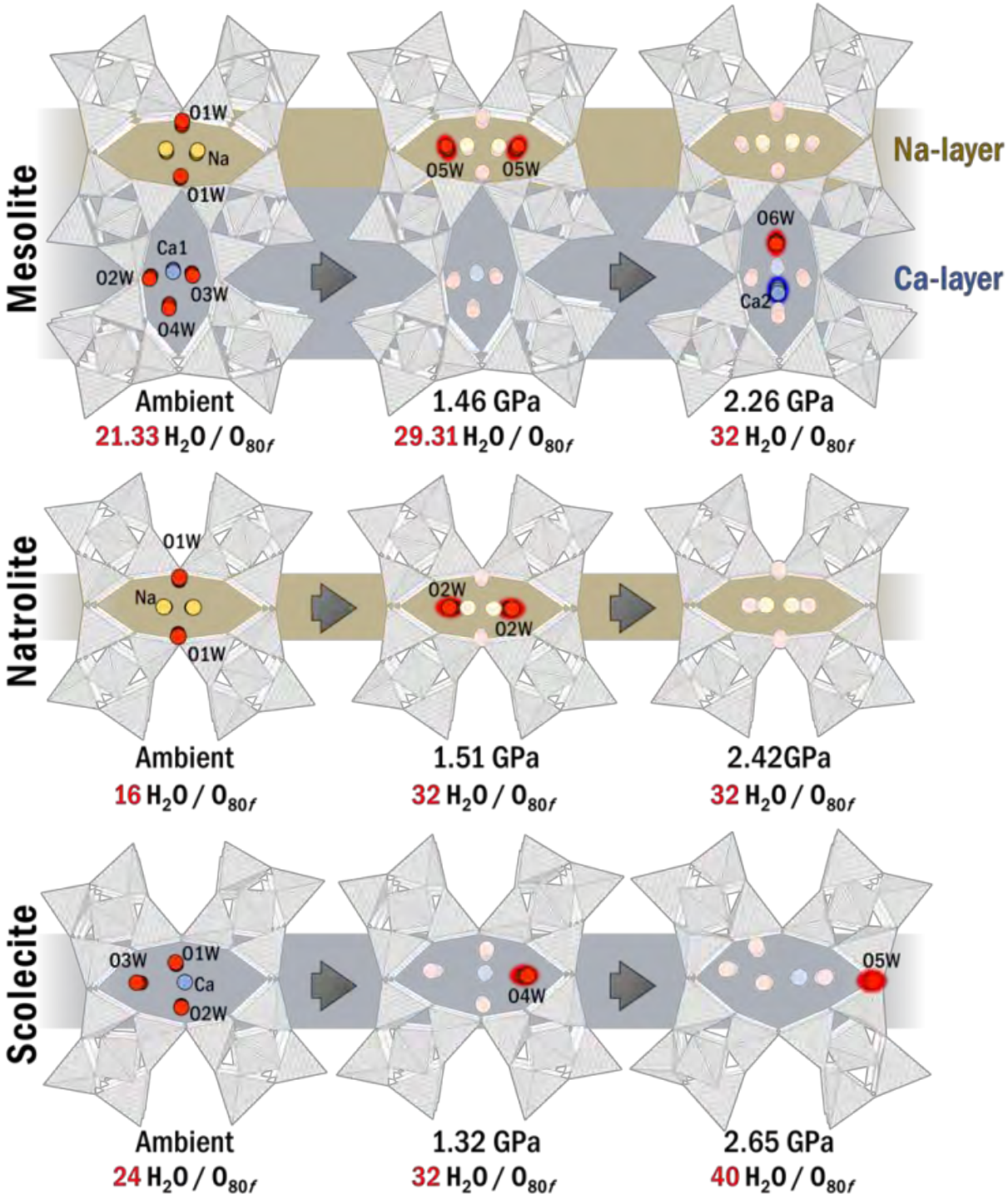

297

298 Fig. 4